

Flynn SL, Szymanowski JES, Dembowski M, Burns PC, Fein JB.  
[Experimental measurements of U24Py nanocluster behavior in aqueous solution.](#)

*Radiochimica Acta* 2016, 104(12), 853-864.

**Copyright:**

©2016 Walter de Gruyter GmbH, Berlin/Boston. This is the authors accepted manuscript that was published in its final definite form by Walter de Gruyter.

**DOI link to article:**

<https://doi.org/10.1515/ract-2015-2493>

**Date deposited:**

19/10/2017

**Embargo release date:**

03 August 2017

1 **Experimental Measurements of U24Py Nanocluster Behavior in Aqueous Solution**

2 **Shannon L. Flynn<sup>1\*</sup>, Jennifer E.S. Szymanowski<sup>1</sup>, Mateusz Dembowski<sup>2</sup>, Peter C. Burns<sup>1, 2</sup>**  
3 **and Jeremy B. Fein<sup>1</sup>**

4 *<sup>1</sup>Department of Civil and Environmental Engineering and Earth Sciences,*  
5 *University of Notre Dame, Notre Dame, IN 46556, USA*

6 *<sup>2</sup>Department of Chemistry and Biochemistry, University of Notre Dame, Notre Dame, IN 46556,*  
7 *USA*

8

9 \* Corresponding Author: [flynn1@ualberta.ca](mailto:flynn1@ualberta.ca)

10

11

## 12 **Summary**

13 Uranyl peroxide nanoclusters may impact the mobility and partitioning of uranium at  
14 contaminated sites and could be used in the isolation of uranium during the reprocessing of  
15 nuclear waste. Their behavior in aqueous systems must be better understood to predict the  
16 environmental fate of uranyl peroxide nanoclusters and for their use in engineered systems. The  
17 aqueous stability of only one uranyl peroxide nanocluster, U60 ( $K_{16}Li_{44}[UO_2(O_2)OH]_{60}$ ), has  
18 been studied to date [1]. In this study, we measured the aqueous stability of a second uranyl  
19 peroxide nanocluster, U24Py ( $Na_{30}[(UO_2)_{24}(O_2)_{24}(HP_2O_7)_6(H_2P_2O_7)_6]$ ), in batch systems as a  
20 function of time, pH, and nanocluster concentration, and then compared the aqueous behavior of  
21 U24Py to U60 to determine whether the size and morphology differences result in differences in  
22 their aqueous behaviors. Systems containing U24Py nanoclusters took over 30 days to achieve  
23 steady-state concentrations of monomeric U, Na, and P, illustrating slower reaction kinetics than  
24 parallel U60 systems. Furthermore, U24Py exhibited lower stability in solution than U60, with  
25 an average of 72% of the total mass in each nanocluster suspension being associated with the  
26 U24Py nanocluster, whereas 97% was associated with the U60 nanocluster in parallel  
27 experiments [1]. The measurements from the batch experiments were used to calculate ion  
28 activity product (I.A.P.) values for the reaction between the U24Py nanocluster and its  
29 constituent monomeric aqueous species. The I.A.P. values, calculated assuming the activity of  
30 the U24Py nanocluster is equal to its concentration in solution, exhibit a significantly lower  
31 nanocluster concentration dependence than those I.A.P. values calculated assuming an activity of  
32 one for the nanocluster. The inclusion of a deprotonation reaction for U24Py minimizes the pH  
33 dependence of the calculated I.A.P. values. The modeling results suggest that the U24Py  
34 nanocluster experiences sequential deprotonation. Taken together, the results indicate that the  
35 aqueous behavior of the U24Py nanocluster, like that of U60, is best described as that of an  
36 aqueous complex.

37 **Keywords:** Nuclear fuel cycle, Uranyl peroxide nanocluster, Aqueous stability, U24Py, U60

38

## 39 1. Introduction

40 Uranyl peroxide nanoclusters represent a class of radionuclide-bearing compounds that  
41 could be present in the environment and may play a role in future radionuclide separation  
42 processes. These nanoclusters could potentially form at contaminated sites such as at Savannah  
43 River, Hanford, and Fukushima [2-3]. Additionally, uranyl peroxide nanoclusters may be used in  
44 an advanced nuclear fuel cycle, as a means of isolating and recycling uranium from nuclear  
45 waste [4-6]. To predict the environmental fate of uranyl peroxide nanoclusters or for their use in  
46 engineered systems, their behavior in aqueous systems must be better understood.

47 Uranyl peroxide nanoclusters are a unique class of uranium materials that rapidly self-  
48 assemble in aqueous solution and are similar in topology to some transition metal  
49 polyoxometalates [4, 7, 8, 9, 10, 11]. The nanoclusters can exist in a crystalline phase composed  
50 of an assemblage of nanoclusters, and as isolated or aggregated nanoclusters in aqueous solution  
51 [1]. In under-saturated solutions, crystals of uranyl peroxide nanoclusters dissolve rapidly to  
52 liberate isolated or aggregated nanoclusters into solution [12]. They have been shown to be at  
53 least metastable in solution, with some persisting for months [2]. Isolated uranyl peroxide  
54 nanoclusters in aqueous solution can be separated from aqueous monomeric species by  
55 ultrafiltration [6]. Flynn et al. [1] examined the aqueous behavior of one type of isolated uranyl  
56 peroxide nanocluster in solution (U60,  $K_{16}Li_{26}[UO_2(O_2)OH]_{60}$ ). In their study, the relationship  
57 between the isolated U60 nanoclusters in solution and simpler uranyl species was found to be  
58 best represented as a dissociation reaction. The calculated ion activity product (I.A.P.) values for  
59 U60 showed the least variation as a function of pH and U60 concentration when U60 was treated  
60 as an aqueous complex with an activity equal to its concentration in solution. It remains unclear  
61 whether the behaviors of all uranyl peroxide nanoclusters in aqueous solution are controlled by  
62 their size, chemical composition, molecular charge in solution, or a combination of these and  
63 possibly other factors.

64 To further understand the behavior of isolated uranyl peroxide nanoclusters in aqueous  
65 solution, this study examines the uranyl peroxide nanocluster U24Py,  
66  $Na_{30}[(UO_2)_{24}(O_2)_{24}(HP_2O_7)_6(H_2P_2O_7)_6]$ . U24Py consists of 24 uranyl peroxide hexagonal  
67 bipyramids that are arranged into six square units in which the uranyl ions are linked by peroxide  
68 bridges. These six square units are linked through pyrophosphate bridges to form an oblate cage  
69 cluster with dimensions of 1.70 nm x 1.89 nm x 1.99 nm [13]. The U24Py nanocluster differs in  
70 composition, shape, and size to U60 nanoclusters. U60 is composed of 60 uranyl peroxide  
71 bipyramids, linked by peroxide and hydroxide bridges to form pentagonal and hexagonal units  
72 that are arranged into a spherical cage with a diameter of 2.4 nm in its crystalline form [7]. The  
73 size of the U24Py and U60 nanoclusters raises a primary question that our research addresses,  
74 whether compounds of this size behave more like bulk solid phases or like large aqueous  
75 complexes. The solubilities of micron-sized particles or larger are independent of particle size;  
76 however, the solubility of smaller particles may increase dramatically with decreasing particle  
77 size. With decreasing particle size, nanoparticle properties, including solubility, are thought  
78 become increasingly dominated by surface free energy effects [14]. According to the Ostwald-  
79 Freundlich equation, particle solubility increases with decreasing particle size for particles less  
80 than approximately 20 nm [15-17]. Flynn et al. [1] demonstrated that the boundary between  
81 aqueous species and solid phases is not a sharp one, and nanoscale materials can exhibit distinct

82 aqueous behaviors from either smaller monomeric aqueous species or bulk solid phases. With  
83 relatively few experimental studies on the aqueous behavior of nanoclusters and nanoparticles in  
84 the sub 10 nm range, our objective was to compare the interactions of U24Py and U60 with  
85 aqueous solutions in order to further our understanding of this transitional behavior.

86 We investigated whether the size and morphology differences between U24Py and U60  
87 lead to differences in their behavior in aqueous solution by measuring the distribution of mass  
88 between U24Py nanoclusters in solution and their constituent monomeric aqueous species as a  
89 function of time, pH, and initial nanocluster concentration. The measured pH and monomeric U,  
90 P, and Na concentrations were used to calculate the I.A.P values for each experiment, accounting  
91 for aqueous speciation of each element in solution. We used the I.A.P. values to test whether the  
92 nanocluster activity in solution affects the calculated I.A.P. value, as would be expected for an  
93 aqueous complex, or if the I.A.P. is independent of the nanocluster activity, analogous to how a  
94 macroscopic solid phase would equilibrate with an aqueous phase. Together with the  
95 corresponding study of U60 [1], this study furthers our understanding of the behavior of uranyl  
96 peroxide nanoclusters in aqueous solution and enhances our ability to predict how these  
97 macromolecules would affect uranium distribution and mobility in environmental and engineered  
98 systems.

## 99 **2. Methods and Materials**

### 100 *2.1. Synthesis and Characterization of Nanoclusters*

101 U24Py crystals were synthesized using a method adapted from Ling et al. [13]. A  
102 solution was prepared by adding 0.5 mL of 0.5 M uranyl nitrate, 0.5 mL of 30% hydrogen  
103 peroxide, and 0.5 mL of 40% tetraethylammonium hydroxide to a 20 mL uncapped glass vial.  
104 After the heat of the reaction dissipated and outgassing stopped, 1.5 mL of 0.1 M sodium  
105 pyrophosphate decahydrate and 1.5 mL of 0.5 M iodic acid were added to the vial. After 14 days,  
106 the U24Py crystals were harvested under vacuum filtration on a Whatman cellulose membrane  
107 with an 11  $\mu\text{m}$  pore size once they reached 2-10 mm. During harvesting the crystals were rinsed  
108 with approximately 5 mL of 18 M $\Omega$  ultrapure water and allowed to dry under vacuum.

109 The purity of samples of the harvested U24Py crystals was tested using a Bruker APEX  
110 X-ray diffractometer with a Mo  $K\alpha$  radiation source. A single crystal was rinsed before being  
111 placed in Infinium oil, and cooled to 110 K for data collection. A complete sphere of data was  
112 collected using four sets of exposures with frame widths of  $0.3^\circ$  in  $\omega$  for each crystal. The  
113 program APEX II was used to correct for polarization and background effects [18], and the  
114 program SHELXTL was used to determine structural solutions [19].

### 115 *2.3. Electrospray Mass Spectrometry*

116 The presence of isolated U24Py nanoclusters within the solutions was verified using  
117 qualitative electrospray ionization mass spectrometry (ESI-MS) at each sampling point. The ESI-  
118 MS spectra were recorded in negative-ion mode with a Bruker micrOTOF-Q II high resolution  
119 quadrupole time of flight mass spectrometer apparatus at the following settings: 3600 V capillary  
120 voltage, 0.4 bar nebulizer gas, 4 L/min dry gas, and 180°C dry gas temperature. The samples  
121 were introduced through direct infusion at 10  $\mu\text{L}/\text{min}$  and scanned over 50-10,000 M/Z with the

122 data averaged over 2-5 minutes. Data was deconvoluted using either standard Bruker large  
123 molecule/protein algorithms or licensed MaxEnt software. Two broad peaks centered at M/Z  
124 values of 1460 and 1600 were determined to be signatures of U24Py. The presence of multiple  
125 peaks is attributed to the creation of multiple charge states of U24Py during ionization due to the  
126 subtraction of differing amounts of Na ions from the U24Py nanocluster. Broad peaks are  
127 commonly observed when large clusters travel through an ionizing field, which strips cations  
128 from the cluster, producing daughters with a similar charge but slightly different masses.

## 129 *2.2. Aqueous Partitioning Experiments*

130 Using a similar method to that reported by Flynn et al. [1], 16 batch partitioning  
131 experiments were conducted at room temperature and pressure (25° C and 1 atm) in an anaerobic  
132 glove box with an atmospheric composition of 95% N<sub>2</sub> and 5% H<sub>2</sub> in order to eliminate  
133 atmospheric CO<sub>2</sub> and the presence of aqueous uranyl carbonate complexes. U24Py suspensions  
134 were prepared in Teflon reaction vessels by dissolving a known mass of U24Py crystals into  
135 18MΩ ultrapure water, which had been bubbled with 95% N<sub>2</sub> and 5% H<sub>2</sub> for 30 minutes. The  
136 complete dissolution of the U24Py crystals was verified in control experiments, in which the  
137 total U concentration did not vary between samples taken from suspensions before and after  
138 passing through a 0.2 μm PTFE membrane (Table S1). Suspensions of U24Py were prepared at  
139 three nanocluster concentrations of approximately 0.9, 1.8, and 2.8 g/L. Suspensions were  
140 adjusted using 1 M LiOH to achieve and maintain pHs of 8.50 ± 0.15, 9.00 ± 0.02, or 9.50 ±  
141 0.01. Each nanocluster concentration and pH experiment was performed at least in duplicate,  
142 with the exception of the pH 9.5, 0.9 g/L and the pH 9.5, 1.8 g/L experiments. A complete table  
143 of experimental conditions is shown in Table S2 in the Supplemental Information. The initial  
144 solutions did not contain monomeric U, P, or Na; therefore, all subsequent measurements of  
145 aqueous monomeric U, P, and Na indicate the dissociation of the U24Py nanoclusters. In the  
146 experimental systems, steady state was only approached from under-saturation with respect to  
147 the U24Py nanoclusters, as a pure yield of U24Py has only been synthesized from polydisperse  
148 solutions.

149 The sealed reaction vessels were rotated at 40 rpm within an anaerobic glove box and  
150 allowed to equilibrate for 24 hours before the first sampling. Sampling was performed,  
151 approximately every 7 day over 47-48 days, within an anaerobic glove box to insure that neither  
152 the experimental systems nor the samples were exposed to atmospheric O<sub>2</sub> or CO<sub>2</sub>. During  
153 sampling, the pH of each experimental system was measured inside the glove box using a  
154 Thermo-Orion Model 420 pH probe with a Thermo-Orion semi-micro glass combo electrode.  
155 The volume of base added and sample removed during sampling was tracked throughout the  
156 duration of the experiments and used to calculate the Li concentration and the ionic strength of  
157 each system at each sampling point. The sample aliquot from each experiment was passed  
158 through a 0.2 μm PTFE membrane to remove any micron-sized precipitates while allowing the  
159 passage of the isolated U24Py nanoclusters as well as monomeric aqueous species. The sample  
160 was subsequently divided into two portions. The first is referred to as ‘before molecular weight  
161 filtration’ (BMWF). The second portion, designated ‘after molecular weight filtration’ (AMWF),  
162 was passed through a 3,000 Da molecular weight sieve, which allowed the passage of  
163 monomeric aqueous species but removed the isolated U24Py nanoclusters (which are 10,051 Da  
164 as isolated nanoclusters in solution, as calculated from the nanocluster stoichiometry)(a

165 schematic of the filtration process is shown in Fig.1) The ability of the molecular weight  
166 filtration to completely separate the U24Py nanoclusters from solution was verified through  
167 control experiments using ESI-MS to detect clusters in solution.

168 The BMWF ESI-MS spectrum contained the two characteristic peaks of the U24Py  
169 nanoclusters; these peaks are absent in the AMWF spectrum, as shown in Fig.2. Therefore, the  
170 elemental composition of the BMWF sample represents the total concentration of each of the  
171 elements in solution, including both the elements present in the U24Py nanoclusters and those  
172 present as monomeric aqueous species. The AMWF elemental composition represents only the  
173 concentration of the monomeric aqueous species that are from the dissolution or dissociation of  
174 the U24Py nanoclusters. The difference between the BMWF and AMWF elemental  
175 concentrations was used to determine the concentration and elemental composition of the U24Py  
176 nanoclusters in solution. Samples collected for U, P, and Na analysis were diluted and acidified  
177 before analysis using inductively coupled plasma optical emission spectroscopy (ICP-OES) (A  
178 detailed description of the ICP-OES methods can be found in the Supplemental Information.

### 179 **3. Results and Discussion**

#### 180 *3.1. Batch Experiments*

181 The measured BMWF concentrations of U, P, and Na did not exhibit a consistent change  
182 as a function of time for the duration of the experiments, as shown by a representative  
183 experiment in Fig. 3A (the complete data set is shown in Figs. S2, S3, and S4 in the  
184 Supplemental Information). The lack of significant variation in the BMWF concentrations as a  
185 function of time indicated that the U24Py crystals rapidly and completely dissolve with no  
186 micron-scale secondary precipitates forming in solution over the duration of the experiments.

187 The AMWF U, P, and Na concentrations slowly increased for the first 28 days of the  
188 experiment and stabilized by Day 34. The AMWF concentrations showed little consistent change  
189 from Day 34 through the termination of the experiments. This indicates that each of the  
190 experimental systems reached a steady-state (Figs. 3B, S5, S6, and S7). The presence of  
191 monomeric U, P, and Na in the AMWF samples indicates unambiguously that the isolated  
192 U24Py nanoclusters dissociate to some extent in solution. The observed perturbations in the  
193 AMWF concentrations after steady-state was achieved were likely due to a combination of  
194 analytical and experimental uncertainties, such as small pH fluctuations between samples and  
195 error associated with the large dilutions required for ICP-OES analyses. Over the course of the  
196 experiment, 21 – 36% of the mass of the nanoclusters was transformed into monomeric aqueous  
197 species. The presence of the two peaks attributed to U24Py throughout the duration of the  
198 experiments in the ESI-MS spectra indicates that the nanoclusters did not completely dissociate  
199 over the sampling period (a representative ESI-MS spectrum from Day 47 is shown in Fig. S1 of  
200 the Supplemental Information).

201 For each experiment, we used the average concentration of the final three sample points,  
202 (from Days 34-48) to represent the AMWF concentration of each element measured at steady-  
203 state under each experimental condition. The measured AMWF U, P, and Na concentrations  
204 exhibited no significant trend as a function of either pH or nanocluster concentration (Figs. 4 and

205 5). The AMWF P/U and Na/U molar ratios averaged over all of the experiments were  $4.01 \pm$   
 206  $0.77$  and  $7.07 \pm 1.45$ , respectively (Fig. 6). These molar ratios showed significant higher  
 207 concentrations of monomeric P and Na in solution when compared to the expected P/U and Na/U  
 208 molar ratios of 1.00 and 1.25, respectively based on the crystalline stoichiometry. Additionally,  
 209 the Na/P ratio in the isolated nanocluster, calculated from the difference between the BMWF and  
 210 AMWF Na and P concentrations, was  $1.26 \pm 0.32$  and approximately equals the 1.25 Na/P ratio  
 211 of crystalline U<sub>24</sub>Py [13]. The higher AMWF concentrations of P and Na relative to the U  
 212 concentration and the nanocluster ratio of Na/P being consistent with the crystalline  
 213 stoichiometry is indicative of one of two scenarios: 1. P and Na were leached congruently from  
 214 the intact nanoclusters, or 2. a secondary submicron-scale U phase that is able to pass through a  
 215 0.2  $\mu\text{m}$  filter membrane and consists of negligible amounts of P or Na precipitated in the  
 216 experimental solutions and. As P is present in the nanocluster as pyrophosphate, the loss of P  
 217 from the nanocluster would result in the loss of the pyrophosphate bridges from the nanocluster  
 218 structure. This loss, in turn, would leave uranyl bipyramids with fewer than their full  
 219 complement of pyrophosphate bridges; it is unlikely that the nanocluster would remain intact  
 220 lacking these integral uranyl pyrophosphate bridges. Hence, with the calculated Na/P ratios in  
 221 the isolated nanoclusters being consistent with the stoichiometric dissolution of the U<sub>24</sub>Py  
 222 nanoclusters, the observed deficit of U in the AMWF solutions is most likely due to precipitation  
 223 of a submicron uranyl phase that is free of P and Na.

### 224 3.2. Metaschoepite Solubility Calculations

225 Thermodynamic modeling was used to determine whether a secondary uranyl phase  
 226 could be buffering the aqueous U concentrations, thereby explaining the observed deficit of U in  
 227 the AMWF calculated P/U and Na/U molar ratios. The most likely known mineral phase that  
 228 could be present at the experimental pH values would be the uranyl hydroxide mineral  
 229 metaschoepite [UO<sub>3</sub>(H<sub>2</sub>O)]. To test whether a metaschoepite phase would be expected to  
 230 precipitate under the experimental conditions, the solubility of metaschoepite was calculated for  
 231 the experimental conditions. The dissolution/precipitation reaction for metaschoepite can be  
 232 expressed as:



234 with the solubility product, K<sub>sp</sub>, represented as:

$$235 K_{\text{sp}} = a_{\text{UO}_2^{+2}} \cdot a_{\text{H}^+} \quad (2)$$

236 where  $a$  represents the thermodynamic activity of the subscripted species, and the activities of  
 237 water and the metaschoepite are taken to be equal to one.

238 The K<sub>sp</sub> value used for these calculations was reported by Gorman-Lewis et al. [20].  
 239 Activity coefficients for the aqueous ions were calculated using the extended Debye-Hückel  
 240 equation with the following constants:  $A = 0.5085$ ,  $B = 0.3281$ ,  $\text{\AA} = 5.22$ , and  $b = 0.02$  [21].



241 RbNO<sub>3</sub> was chosen as the most reasonable species for approximating the values of  $\tilde{a}$  and  $\tilde{b}$  based  
242 on cation size, as these values have yet to be determined for a uranyl-dominated system. For the  
243 purpose of calculating the expected metaschoepite solubility under the experimental conditions,  
244 the ionic strength was estimated as 0.0069 M. The standard-states used for solid phases and for  
245 H<sub>2</sub>O are the pure mineral or fluid, respectively, at the pressure and temperature of interest. For  
246 aqueous species, the standard-state is defined as a hypothetical one molal solution that behaves  
247 as if it is infinitely dilute. Activity coefficients of neutral aqueous species were assumed to be  
248 equal to one in the calculations. The Na and P concentrations were taken to be equal to the  
249 average of the final three sampling points of the measured AMWF concentration for all of the  
250 U<sub>24</sub>Py experiments, yielding values of 10<sup>-2.71</sup> and 10<sup>-2.97</sup> M, respectively. The total aqueous  
251 peroxide concentration in solution was assumed to be equal to the average total AMWF P  
252 concentration because of the 1:1 ratio of peroxide:P in the U<sub>24</sub>Py nanocluster. This ratio was  
253 deemed a better proxy for the peroxide concentration than uranium, as the precipitation of a  
254 secondary uranium phase would result in under-estimation of the peroxide concentration.

255 Uranium speciation was calculated by determining the activities of all aqueous species  
256 for all elements using a system of nonlinear mass action [20, 22, 23, 24] (Table S.3) and mass  
257 balance equations using a Newton-Raphson iteration program. The total uranium concentration  
258 (the sum of the individual aqueous uranium species) in equilibrium with metaschoepite as a  
259 function of pH is depicted in Fig. 7, and compared with the average of the AMWF U  
260 concentrations for the final three sampling points of each experiment. The measured AMWF U  
261 concentrations were approximately equal to or exceeded the expected solubility of metaschoepite  
262 under the experimental conditions, indicating that conditions are favorable for metaschoepite  
263 precipitation under experimental conditions. The super-saturated state with respect to  
264 metaschoepite and the deviation of the Na/U and P/U AMWF molar ratios suggests that a  
265 metaschoepite-like phase precipitated. Due to the likely presence of metaschoepite in the  
266 experimental systems, for the subsequent I.A.P. calculations, we assumed that the measured  
267 aqueous U concentrations are in equilibrium with an amorphous metaschoepite-like phase and  
268 that the isolated U<sub>24</sub>Py nanocluster in solution has the same stoichiometry as the U<sub>24</sub>Py  
269 crystalline phase reported by Ling et al. [13] of Na<sub>30</sub>[(UO<sub>2</sub>)<sub>24</sub>(O<sub>2</sub>)<sub>24</sub>(HP<sub>2</sub>O<sub>7</sub>)<sub>6</sub>(H<sub>2</sub>P<sub>2</sub>O<sub>7</sub>)<sub>6</sub>].

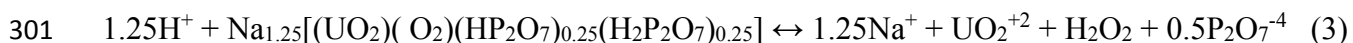
### 270 *3.3. Determination of Aqueous Behavior: Ion Activity Product Calculations*

271 If the reaction for the dissolution or dissociation of the U<sub>24</sub>Py nanocluster was properly  
272 described and if U<sub>24</sub>Py nanoclusters reached equilibrium or at least a steady-state with the  
273 monomeric aqueous species in the experimental solutions, then the ion activity product can be  
274 calculated from each set of measured concentrations. The calculated I.A.P. should be equivalent  
275 to the equilibrium constant and should not vary as a function of pH or nanocluster concentration.  
276 The calculation of the I.A.P. for the U<sub>24</sub>Py nanocluster has two unknowns: 1) the reaction  
277 stoichiometry, and 2) the nature and behavior of the nanocluster in solution.

278 As described in the previous section, the crystalline phase stoichiometry was used to  
279 represent the stoichiometry of the isolated nanoclusters in solution, and we assumed that once the  
280 solution reached steady-state that the solution was simultaneously in equilibrium with both the  
281 isolated nanoclusters and a metaschoepite-like phase. The U<sub>24</sub>Py nanocluster could behave in  
282 solution either as a solid phase or as an aqueous complex. A solid phase would exhibit a

283 solubility that is independent of the concentration of the solid phase as long as the solid is  
 284 present in excess. Therefore, if the dispersed U24Py nanoclusters in solution behave like a pure  
 285 solid, then their activity would be equal to one, and the I.A.P. values calculated under that  
 286 assumption should be equivalent to the equilibrium constant for the dissolution reaction and  
 287 should be independent of pH and nanocluster concentration. In contrast, if the U24Py behaves  
 288 like an aqueous complex, then the calculated I.A.P. value would only be independent of pH and  
 289 nanocluster concentration when the activity or concentration of the U24Py is accounted for. The  
 290 nature of the nanocluster behavior in solution was characterized by calculating the I.A.P. values  
 291 using both approaches, and then determining which approach yields the lowest dependence on  
 292 pH and nanocluster concentration.

293 The protonation state of U24Py affects the stoichiometry of the reaction between isolated  
 294 nanoclusters and monomeric aqueous species, however the protonation state of the nanocluster in  
 295 solution is unknown and likely varies with pH. Therefore, we initially assumed that the  
 296 nanocluster is fully protonated. Subsequently, different protonation states for the nanocluster  
 297 were tested as a means to yield I.A.P. values that do not change with pH or nanocluster  
 298 concentration. For the purpose of calculating the I.A.P. value, a simplified stoichiometry based  
 299 on a single uranyl peroxide pyrophosphate unit was used that, maintains the same stoichiometric  
 300 ratios as the entire U24Py nanocluster yielding the following dissolution/dissociation reaction:



302 The I.A.P. for Reaction (3) can be expressed as:

$$303 \quad \text{I. A. P.} = \frac{a_{\text{Na}^+}^{1.25} \cdot a_{\text{UO}_2^{+2}} \cdot a_{\text{H}_2\text{O}_2} \cdot a_{\text{P}_2\text{O}_7^{-4}}^{0.5}}{a_{\text{H}^+}^{1.25} \cdot a_{\text{U24Py Nanocluster}}} \quad (4)$$

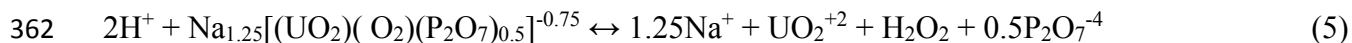
304 where  $a$  represents the thermodynamic activity of the subscripted species, and  $a_{\text{U24Py Nanocluster}}$   
 305 represents the activity of the U24Py nanocluster in solution (see below). The I.A.P. values for  
 306 Reaction (3) were calculated using a similar computational approach to that used to calculate the  
 307 solubility of metaschoepite, but with the ionic strength calculated for each experiment in order to  
 308 determine the activity coefficient for each species. The ionic strength was found to vary from  
 309 0.0031-0.0069 M with no systematic variation by either pH or nanocluster concentration.

310 The activities of the aqueous species in Eq. (4) were calculated by solving a system of  
 311 nonlinear mass action (Tables S.3. and S.4.) and mass balance equations in which the total  
 312 aqueous U, P, and Na concentrations were the average measured AMWF concentration from the  
 313 final three sampling points for each experiment and the Li concentration was calculated from the  
 314 amount added while adjusting the experimental pHs. The activity of  $\text{H}_2\text{O}_2$  was assumed to be  
 315 equal to the measured AMWF P concentration as the U24Py structure contains pyrophosphate  
 316 and peroxide as integral bridging ligands. Therefore, for every mole of P liberated from the  
 317 nanoclusters, a mole of peroxide would also have to be liberated. Peroxide is miscible in water  
 318 and does not exsolve from the suspension at the concentrations in the experiments. Peroxide  
 319 reduction was not expected to occur to a significant extent due to the short duration of the  
 320 experiments and the lack of species present in the experimental systems that are readily oxidized.  
 321 If the peroxide was unstable and a significant portion of the peroxide was reduced during the

322 experiment, then Reaction (3) would be driven to the right continually over the course of the  
323 experiments. The solutions would not have reached equilibrium or steady-state with respect to  
324 dissolved U, P, or Na, and the steady-state that we observed in the AMWF concentrations of U,  
325 P and Na after 34 days would not have occurred. The nanocluster concentration for the  
326 speciation calculations was calculated from the difference between the measured BMWF and  
327 AMWF P concentrations, which is equal to the difference between the total element and aqueous  
328 concentrations. As the experiments were conducted in an anaerobic glove box, aqueous  
329 carbonate species were excluded from the calculations.

330 The concentration and pH dependencies of the I.A.P. values calculated assuming the  
331 U24Py nanocluster is fully protonated with either an activity of one or an activity equal to the  
332 nanocluster concentration are shown in Figure 8. Both sets of calculated I.A.P. values show a  
333 weak concentration dependence over the examined U24Py concentration range. The I.A.P.  
334 values calculated treating the U24Py nanoclusters as an aqueous complex exhibit less of a  
335 concentration dependence (with a slope of -0.14) than the I.A.P. values calculated assuming that  
336 the U24Py behaves as a bulk solid (with a slope of -0.35). Both methods of calculating the I.A.P.  
337 values exhibit a strong pH dependence across the pH range of the experiments. The I.A.P. values  
338 calculated treating the U24Py nanocluster as an aqueous complex have a slope of -0.88; the  
339 I.A.P. values calculated treating U24Py nanocluster as a bulk solid have a slope of -0.84. The  
340 relatively large slope as a function of pH for both models indicates that the reaction as written  
341 does not properly account for the proton condition of the U24Py nanocluster, further suggesting  
342 that the nanocluster is at least partially deprotonated in solution under the experimental  
343 conditions.

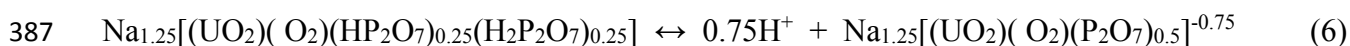
344 We used our data to place constraints on the protonation behavior of the U24Py  
345 nanocluster in solution by determining the extent of deprotonation that is required to yield I.A.P.  
346 values that do not vary with pH or nanocluster composition. First, we tested a model in which the  
347 U24Py nanoclusters are assumed fully deprotonated and remain fully deprotonated across the pH  
348 range of the experiment. Second, we tested a model that uses a single cumulative deprotonation  
349 reaction to account for changing protonation state as a function of pH under the experimental  
350 conditions. Each pyrophosphate unit in the U24Py nanocluster has four oxygen bonds with  
351 uranyl bipyramids, leaving two terminal oxygen atoms available for protonation. Each U24Py,  
352 therefore, has 24 potential proton active sites. Ling et al. [13] determined that at least six of these  
353 sites have Na atoms bound to them, leaving 18 terminal oxygen atoms available for  
354 deprotonation. Under the assumption that the U24Py nanocluster is fully deprotonated, it would  
355 have a charge of -18 in solution, and if the Knud Thomsen formula is used to approximate the  
356 surface area of the oblate nanocluster, then the calculated charge density of the U24Py  
357 nanocluster would be 241 mC/m<sup>2</sup>. A charge of -18 and a charge density of 241 mC/m<sup>2</sup> is not  
358 unreasonable for this size of nanocluster, as the charge of U60 in solution has been determined to  
359 be -19 with a charge density of 159 mC/m<sup>2</sup> [1]. The -18 charge of the entire U24Py nanocluster  
360 translates to a charge of -0.75 for the simplified nanocluster stoichiometry. The dissolution or  
361 dissociation reaction for the fully deprotonated U24Py nanocluster is written as:



363 Even with the use of unrealistic values for the ion size parameter  $\text{\AA}$  and the empirical term  
 364  $\text{cI}$  as a correction factor, Czap et al. [25] found that the extended Debye-Hückel equation fails to  
 365 account for the non-ideal behavior of nanoscale tungstoaluminate polyoxometalates (POMs) in  
 366 solution. POMs cannot be treated as point charges as required by Debye-Hückel theory [25-27]  
 367 due to their relatively large size as compared to simple aqueous ions that the theory is based on.  
 368 Therefore, for all subsequent calculations, we assumed that the activity of the U24Py  
 369 nanoclusters is equal to their concentration in solution and that the nanoclusters do not contribute  
 370 to the solution ionic strength.

371 Both the concentration and pH dependencies of the I.A.P. values are reduced when the  
 372 U24Py nanocluster was assumed to be fully deprotonated (Fig. 9). The I.A.P. values that were  
 373 calculated by treating the U24Py nanocluster as a bulk solid show a more significant  
 374 concentration dependence (with a slope of -0.27) than those that were calculated treating the  
 375 nanocluster as an aqueous complex (with a slope of -0.07). The I.A.P. values from both  
 376 calculations show a significant decrease in their pH dependence when the U24Py nanocluster is  
 377 assumed to be fully deprotonated compared to the fully protonated I.A.P. values. The I.A.P.  
 378 values calculated by treating the U24Py nanocluster as an aqueous complex have a slope versus  
 379 pH of -0.14; the I.A.P. values calculated by treating U24Py nanocluster as a bulk solid have a  
 380 slope of -0.09.

381 The complete deprotonation of the U24Py nanocluster involves 18 proton reactive sites,  
 382 where each is likely characterized by a different proton affinity and distinct acidity constant, or  
 383  $K_a$  value. Constraining the  $K_a$  value for all 18 deprotonation reactions is beyond the precision of  
 384 our data. Instead we tested a model in which U24Py is not fully deprotonated across the pH  
 385 range of the experiments by approximating this behavior by invoking a complete deprotonation  
 386 reaction, as expressed by:



388 where the acidity constant can be written:

$$389 K_a = \frac{a_{\text{H}^+}^{0.75} \cdot a_{\text{U24Py Nanocluster } -0.75\text{H}^+}^{-0.75}}{a_{\text{U24Py Nanocluster}}} \quad (7)$$

390 where  $a_{\text{U24Py Nanocluster}}$  represents the activity of the fully protonated U24Py nanocluster and  
 391  $a_{\text{U24Py Nanocluster } -0.75\text{H}^+}$  represents the activity of the fully deprotonated U24Py nanocluster in  
 392 solution. If the addition of Reaction (6) to the system of equations used to determine the I.A.P.  
 393 values further reduces the pH dependence of the calculated I.A.P. values, then our results would  
 394 suggest that the U24Py nanocluster exhibits deprotonation behavior as a function of pH. It may  
 395 not exist exclusively as either fully protonated or fully deprotonated molecules, as suggested by  
 396 Reaction (6). In fact, the molecule is unlikely to do so. However, the results would suggest that  
 397 multiple protonation states are needed to account for the observed behaviors as a function of pH  
 398 and nanocluster concentration.

399 For this test, we could not simultaneously solve for both the  $K_a$  value in Eq. (7) and the  
 400 I.A.P. value for Reaction (3). Therefore, we used an iterative procedure to solve for the I.A.P.

401 values, assuming different fixed values for the  $K_a$ , and we determined which  $K_a$  value yields the  
402 least dependence of the I.A.P. value as a function of pH and nanocluster concentration. These  
403 tests reveal that the pH dependence is minimized when the  $K_a$  value is equal to -3.5.

404 The addition of the deprotonation reaction yields I.A.P. values with lower concentration  
405 and pH dependencies than those calculated assuming that the nanocluster is either fully  
406 protonated or fully deprotonated exclusively (Fig. 10). Treating the nanocluster as a bulk solid  
407 results in a larger slope of the I.A.P. values as a function of nanocluster concentration compared  
408 to treating the nanocluster as an aqueous complex: -0.27 and -0.07, respectively. The addition of  
409 the U24Py deprotonation reaction yields I.A.P. values for both sets of calculations that are close  
410 to being independent of the experimental pH. The slope of the I.A.P. values assuming that the  
411 nanocluster behaves as a bulk solid is -0.09, while treating the nanocluster as an aqueous  
412 complex yields a slope of -0.13.

413 Although neither of the calculation approaches yields I.A.P. values that are completely  
414 independent of nanocluster concentration, the approach that treats the isolated U24Py  
415 nanoclusters as aqueous complexes yields I.A.P. values that are significantly closer to being  
416 independent of nanocluster concentration than those calculated by treating the nanocluster as a  
417 bulk solid with an activity of one. In order to reduce the pH dependence of the calculated I.A.P.  
418 values, the deprotonation behavior of the U24Py nanocluster must be accounted for with the  
419 addition of a deprotonation reaction for the nanocluster. A conditional estimate of the  
420 equilibrium constant can be made by averaging all of the I.A.P. values that were calculated  
421 treating the nanocluster with a non-unit activity (Fig. 10), yielding a value of  $-5.0 \pm 0.1 / -0.2 (1\sigma)$   
422 for the log equilibrium constant for Reaction 3. Our modeling results strongly suggest that the  
423 U24Py nanocluster experiences deprotonation over the experimental pH range, and that the  
424 nanoclusters are mostly deprotonated across the pH range of the experiments. Taken together,  
425 the results indicate that the aqueous behavior of the U24Py nanocluster is best described as that  
426 of an aqueous complex that undergoes sequential deprotonation as a function of pH.

427 Even though U24Py and U60 are both uranyl peroxide nanoclusters, we observed several  
428 differences in their aqueous behavior. In the U60 experiments [1], a steady-state between the  
429 isolated nanoclusters and monomeric aqueous species was attained within 24 hours. The U24Py  
430 experiments took over 30 days to attain a steady-state, illustrating much slower overall reaction  
431 kinetics that might be partly due to the formation of a secondary amorphous metaschoepite  
432 phase. The U24Py nanoclusters also exhibited lower stability, with an average of 72% of the  
433 total mass in the system being associated with the nanoclusters, whereas an average of over 97%  
434 was associated with the U60 nanoclusters under similar experimental conditions. The mass  
435 associated with the U24Py likely would be even lower if the U24Py experiments were conducted  
436 open to the atmosphere and subjected to the formation of uranyl-carbonate complexes as was the  
437 case in the U60 experiments. The difference between the U60 and U24Py experiments means  
438 that the reported difference in nanocluster stabilities is likely a minimum value, and direct  
439 comparison of the relative stabilities is difficult. Both types of nanoclusters are highly charged in  
440 solution. U60 exhibits a molecular charge of -19 with a charge density of  $159 \text{ mC/m}^2$ , which is  
441 caused by the leaching of  $\text{Li}^+$  cations from the nanocluster, and the charge does not vary  
442 significantly with pH [1]. Conversely, the maximum charge of U24Py is -18 with a charge

443 density of  $241 \text{ mC/m}^2$ , likely caused by the deprotonation of the nanocluster, and is therefore  
444 dependent on pH. The greater charge density of the isolated U24Py nanocluster likely contributes  
445 to U24Py exhibiting a lower stability in aqueous solution than U60. However, for both U24Py  
446 and U60, the calculated I.A.P. values yield lower pH and nanocluster dependencies when treated  
447 as aqueous complexes with non-unit activities than when treated as bulk solids with activities  
448 equal to one. The results of these two studies indicate that uranyl peroxide nanoclusters such as  
449 U24Py and U60 are highly charged species when present in solution, whose aqueous behavior is  
450 best described as that of an aqueous complex. The conclusion that U24Py and U60 nanoclusters  
451 are best modeled as aqueous complexes with non-unit activities is consistent with theoretical  
452 work that has concluded that the behavior of a nanoparticle in solution is dominated by the  
453 behavior of the surface atoms [28]. As the size of a particle decreases, the proportion of surface  
454 atoms to total atoms in the particle increases to a point where the surface atoms dominate the  
455 overall chemical potential of the particle resulting in behaviors that differ from macroscopic bulk  
456 solids of the same elemental composition. Uranyl-peroxide nanoclusters such as U24Py and U60  
457 can be considered to consist entirely of surface atoms, and hence they do not exhibit bulk solid  
458 phase behavior.

#### 459 **4. Conclusions**

460 In this study, the stability and aqueous behavior of U24Py nanoclusters were determined  
461 as a function of time, pH, and nanocluster concentration. Systems with U24Py suspended in  
462 solution achieved a steady-state between the U24Py nanoclusters and aqueous monomeric  
463 species after approximately 34 days, and this steady-state was maintained for at least 14 days.  
464 The measured AMWF concentrations did not vary systematically as a function of pH or  
465 nanocluster concentration over the ranges examined. The I.A.P. values that were calculated  
466 assuming activities of the nanoclusters equal to their concentration in solution exhibit  
467 significantly lower nanocluster concentration dependence than those calculated assuming an  
468 activity of one for the nanocluster. The addition of a complete deprotonation reaction for the  
469 U24Py nanocluster minimizes the pH dependence of the calculated I.A.P. values. Our modeling  
470 results strongly suggest that the U24Py nanocluster experiences deprotonation and that the  
471 nanoclusters are mostly deprotonated across the pH range of the experiments. Taken together,  
472 the results indicate that the aqueous behavior of the U24Py nanocluster is best described as that  
473 of an aqueous complex that undergoes sequential deprotonation as a function of pH.

474 U24Py and U60 are just two uranyl peroxide nanoclusters in a family of more than 55 published  
475 structures. Further characterization of how nanocluster size, composition and morphology affect  
476 aqueous solution behavior is needed in order to construct general models of the behavior of  
477 uranyl peroxide and other nanoclusters, and to better understand the distribution and fate of  
478 metal and radionuclides in aqueous systems that contain nanoclusters.

#### 479 **Acknowledgements**

480 This work was supported as part of the *Materials Sciences of Actinides* Center, an Energy  
481 Frontier Research Center funded by the U.S. Department of Energy, Office of Science, Office of  
482 Basic Energy Sciences under Award Number DE-SC0001089. ICP-OES analyses were  
483 conducted at the Center for Environmental Science and Technology at the University of Notre

484 Dame. Electrospray Mass Spectrometry was performed in the Mass Spectrometry and  
485 Proteomics Facility at the University of Notre Dame supported by the National Science  
486 Foundation (CHE-0741793). We would like to thank the journal reviewer whose comments  
487 significantly improved this manuscript.

## 488 **References**

- 489 1. Flynn S.L., Szymanowski J.E.S., Gao Y., Liu T.; Burns P.C., Fein J.B.: Experimental  
490 measurements of U60 nanocluster stability in aqueous solution. *Geochemica et Cosmochimica*  
491 *Acta* **156**, (2015).
- 492 2. Armstrong C. R., Nyman M., Tatiana S., Sigmon G. E., Burns P. C., Navrotsky A.: Uranyl  
493 peroxide enhanced nuclear fuel corrosion in seawater. *PNAS* **109**, 6 (2012).
- 494 3. Burns P.C., Ewing R.C., Navrotsky A.: Nuclear fuel in a reactor accident. *Science* **335**, 1184  
495 (2012).
- 496 4. Liao Z., Deb T., and Nyman M.: Elucidating self-assembly mechanisms of uranyl-peroxide  
497 capsules from monomers. *Inorg. Chem.* **53**, 19 (2014).
- 498 5. Miro P., Vlaisavljevich B., Dzubak A.L., Hu S., Burns P.C., Cramer C.J., Spezia R., Gagliardi  
499 L.: Uranyl-peroxide nanocapsules in aqueous solution: force field development and first  
500 applications. *J. Phys. Chem.* **118**, 42 (2014).
- 501 6. Wylie E.M., Peruski K.M., Weidman J.L., Phillip W.A., Burns P.C.: Ultrafiltration methods of  
502 uranyl peroxide nanoclusters for the separation of uranium from aqueous solutions. *ACS Appl.*  
503 *Mater. Interfaces* **6**, 1 (2014).
- 504 7. Sigmon G.E., Ling J., Unruh D.K., Moore-Shay L., Ward M., Weaver B., Burns P.C.: Uranyl-  
505 peroxide interaction favor nanocluster self-assembly. *J. Am. Chem. Soc.* **131**, 46 (2009a).
- 506 8. Sigmon G.E., Unruh D.K., Ling J., Weaver B., Ward M., Pressprich L., Simonetti A., Burns  
507 P.C.: Symmetry versus minimal pentagonal adjacencies in uranium-based polyoxometalate  
508 fullerene topologies. *Angew. Chem. Int. Ed.* **48**, 15 (2009b).
- 509 9. Nyman M., Rodriguez M.A., Campana C.F.: Self-assembly of alkali-uranyl-peroxide clusters.  
510 *Inorg. Chem.* **131**, 17 (2010).
- 511 10. Sigmon G.E., Burns P.C.: Rapid self-assembly of uranyl peroxide polyhedral into crown  
512 clusters. *J. Am. Chem. Soc.* **133**, 24 (2011).
- 513 11. Qui J., Burns P.C.: Cluster of actinides with oxide, peroxide, or hydroxide bridges. *Chem.*  
514 *Rev.* **113**, 2 (2013).

- 515 12. Qui J., Ling, J., Sui, A., Szymanowski, J.E.S., Simonetti, A., Burns P.C.: Time resolved self-  
516 assembly of a fullerene-topology core-shell cluster containing 68 uranyl polyhedra. *J. Am.*  
517 *Chem. Soc.* **134**, 3 (2012).
- 518 13. Ling J., Qiu J., Sigmon G.E., Ward M., Szymanowski J.E.S., Burns P.C.: Uranium  
519 pyrophosphate/methylenediphosphate polyoxometalate cage clusters. *J.A.C.S.* **132**, 38 (2010).
- 520 14. Navrotsky A.: Energetics of nanoparticle oxides: interplay between surface energy and  
521 polymorphism. *Geochem. Trans.* **4**, 6 (2003).
- 522 15. Gilbert B., and Banfield J.F.: Molecular-scale processes involving nanoparticulate minerals  
523 in biogeochemical systems. *Reviews in Minerology and Geochemistry* **59**, 1 (2005)
- 524 16. Johnson K.C.: Comparison of methods for predicting dissolution and the theoretical  
525 implications of particle size dependent solubility. *J. Pharmaceutical Sci.* **101**, 2 (2012).
- 526 17. Kaptay G.: On the size and shape dependence of the solubility of nano-particles in solutions.  
527 *Internat. J. Pharmaceutics* **430**, 1 (2012).
- 528 18. Bruker: SADABS. Bruker AXS Inc., Madison, WI 2001.
- 529 19. Sheldrick, G. M.: SHELX-97 Program pack or solution and refinement of crystal structures  
530 from x-ray diffraction data, Bruker AXS, Inc. Madison, WI 1997.
- 531 20. Gorman-Lewis D., Fein J.B., Burns P.C., Szymanoski J.E.S., Converse J.: Solubility  
532 measurements of uranyl oxide hydrate phases metaschopite, compregnacite, Na-compregnacite,  
533 becquerelite and clarkite. *J. Chem. Thermodynamics* **40**, 6 (2008).
- 534 21. Helgeson H. C., Kirkham D. H., Flowers G. C.: Theoretical prediction of the thermodynamic  
535 behavior of aqueous-electrolytes at high pressures and temperatures. 4. Calculation of activity-  
536 coefficients, osmotic coefficients, and apparent molal and standard and relative partial molal  
537 properties to 600-degrees-C and 5 kb. *Am. J. Sci.* **281**, (1981).
- 538 22. Martell R.J. and Smith R.M.: NIST Critical selected stability constants of metal complexes,  
539 Version 6.0, NIST Standard Reference Database 462001, National Institute of Standards and  
540 Technology; Gaithersburg, MD 2001.
- 541 23. Guillaumont R., Fanghanel T., Fuger J., Grenthe I., Neck V., Palmer D., Rand M.: Updated  
542 on the Chemical Thermodynamics of Uranium, Neptunium and Plutonium, second  
543 ed., Elsevier; Amsterdam 2003.
- 544 24. Zaninato P.L., Di Bernardo P., Grenthe I.: Chemical equilibria in the binary and ternary  
545 uranyl(VI)-hydroxide-peroxide systems. *Dalton Trans.* **41**, 12 (2012).



- 546 25. Czap A., Neuman N.I., Swaddle T.W.: Electrochemistry and homogeneous self-exchange  
547 kinetics 12-tungstoaluminate (5-/6-) couple. *Inorg. Chem.* **45**, 23 (2006).
- 548 26. Liu, T.B.: Hydrophilic Macroionic Solutions: What happens when soluble ions reach the size  
549 of nanometer scale? *Langmuir* **26**, 12 (2010).
- 550 27. Haso F., Fang X., Yin P., Ross J.L., Liu T.: The self-assembly of a macroion with anisotropic  
551 surface charge density distribution. *Chem. Commun.* **49**, 6 (2013).
- 552 28. Rusanov A. I., Shchekin A.K.: On the formulation of the material equilibrium condition for a  
553 dissolving solid nanoparticle. *A.I.P.* **127**, 19 (2007).

554 **Figure 1.** Schematic of experimental filtration process. 1) 0.2  $\mu\text{m}$  PTFE membrane used to test  
555 for secondary microscale particulates. 2) 3,000 Da molecular weight filter to separate the  
556 nanocluster from the monomeric aqueous species. All samples were divided into two portions for  
557 the analysis of U, P and Na: (A) Before molecular weight filtration (BMWF) which measured the  
558 element concentrations after filtration step 1, but before filtration step 2; and (B) the After  
559 molecular weight filtration (AMWF) which measured the element concentrations after molecular  
560 weight filtration, step 2.

561 **Figure 2.** Representative electrospray mass spectroscopy spectra plotted on an arbitrary y-axis.  
562 The spectrum from the BMWF sample is represented by the solid curve, and the spectrum from  
563 the AMWF spectrum is represented by the dashed curve.

564 **Figure 3.** An example of U24Py nanocluster partitioning experiments from experiment S22,  
565 conducted under the following conditions: pH 8.7 and 2.86 g/L U24Py. Remaining experimental  
566 data are shown in the Supplemental Information section. **A)** BMWF concentrations of U, P, and  
567 Na; **B)** AMWF concentrations of U, P, and Na.

568 **Figure 4.** Measured AMWF **A)** U, **B)** P, and **C)** Na concentrations from all experiments. Each  
569 data point represents the average concentration of the final three data points for a particular  
570 experiment. A, B, and C are plotted as a function of final solution pH for U, P, and Na,  
571 respectively.

572 **Figure 5.** Measured AMWF **A)** U, **B)** P, and **C)** Na concentrations from all experiments. Each  
573 data point represents the average concentration of the final three data points for a particular  
574 experiment. A, B and C are plotted as a function of initial nanocluster concentration in each  
575 experiment for U, P and Na, respectively.

576 **Figure 6.** The calculated AMWF **A)** Na/U and **B)** P/U molar ratios from all experiments. Each  
577 data point represents the molar ratio calculated from the average concentration of the final three  
578 data points for a particular experiment.

579 **Figure 7.** The average AMWF uranium concentrations in the final three data points from each  
580 experiment ( $\circ$ ) plotted with the calculated solubility of metaschoepite as the solid curve.

581 **Figure 8.** Calculated I.A.P. values assuming the U24Py nanocluster is fully protonated. The  
582 diamonds represent the I.A.P values calculated by treating the nanoclusters as a solid phase with  
583 an activity of one. The circles represent the I.A.P. values calculated by treating the nanoclusters  
584 as aqueous complexes with an activity equal to the nanocluster concentration in solution. **A)**  
585 I.A.P. values as a function of nanocluster concentration. **B)** I.A.P. values as a function of pH.  
586 Lines are linear best-fits of each set of values.

587 **Figure 9.** Calculated I.A.P. values assuming the U24Py nanocluster is fully deprotonated as a  
588 function of: **A)** nanocluster concentration; and **B)** pH. Lines are linear best-fits of each set of  
589 values. Data symbols are the same as in Figure 8.

590 **Figure 10.** Calculated I.A.P. values incorporating a U24Py deprotonation reaction in the  
591 calculations. **A)** I.A.P. values as a function of nanocluster concentration **B)** I.A.P. values as a

592 function of pH. Lines are linear best-fits of each set of values. Data symbols are the same as in  
593 Figure 8.